



ELEG 404/604 - Digital Image and Audio  
Signal Processing

Computed Tomography

Gonzalo R. Arce

Charles Black Evans Professor

Department of Electrical and Computer Engineering  
University of Delaware

Spring 2014

# X-Ray discovery\*

In 1895 Wilhelm Rontgen discovered the X-rays, while working with a cathode ray tube in his laboratory. One of his first experiments was a film of his wife's hand.



\*Based on slides from Mark Miroznik (ELEG 679)

# Shoe Fitting X-Ray Device

Shoe stores in the 1920s until the 1970s installed X-ray fluoroscope machines as a promotion device.

**CERTIFICATE**

SHOE-FITTING TEST DATA FOR \_\_\_\_\_

1. ANKLE ROLL    GOOD     FAIR     POOR

2. WEIGHT DISTRIBUTION

LEFT    RIGHT

—% BALL    —%  
—% OUTER    —%  
—% HEEL    —%

RIGHT WAY    WRONG WAY

3. X-RAY FITTING TEST

LEFT    RIGHT

—% GOOD    —%  
—% FAIR    —%  
—% POOR    —%

RIGHT WAY    WRONG WAY

**SCIENTIFIC SHOE FITTING AT ITS BEST**

On Dr. Scholl's Shoe X-ray you can see the position of the bones in your feet right through the shoe. In addition to this checkup other methods of scientific shoe fitting will be employed here during this special demonstration.

**This scientific way of approaching the problem of poorly-fitted shoes eliminates guesswork. Now you can see for yourself!**

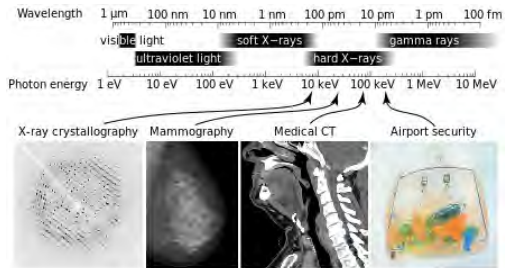
Oak Ridge Associated Universities  
Shoe-Fitting Fluoroscope [ca. 1930-1940]

**Dr. Scholl's** SHOE FITTING EXPERTS FROM THE CHICAGO FACTORY  
will be in our store  
Monday, February 15th

They bring with them the complete line of Dr. Scholl's Shoes (822 fittings) . . . every size, width and style . . . for every type foot. X-ray fitting—as well as other Dr. Scholl shoe fitting devices. Now you can obtain the shoe that will give you perfect satisfaction—and if you have foot troubles you will be shown how to obtain relief, quickly and inexpensively. Be sure to attend this great DISPLAY and DEMONSTRATION . . . first of its kind in this city.

**GEO. S. MERCHANT**  
Winter Garden, Fla.

# X-Ray Spectrum



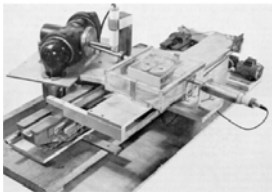
$$E = \hbar \cdot f = \hbar \frac{c}{\lambda}.$$

1 eV is the kinetic energy gained by an electron that is accelerated across a one volt potential.

- **Wavelength:** 0.01 - 10 nm.
- **Frequency:** 30 petahertz ( $3 \times 10^{16}$ ) to 30 exahertz ( $3 \times 10^{19}$ ).
- **Soft X-Rays:** 0.12 to 30 keV.
- **Hard X-Rays:** 30 to 120 keV.

# Reconstruction History

Hounsfield's experimental CT:

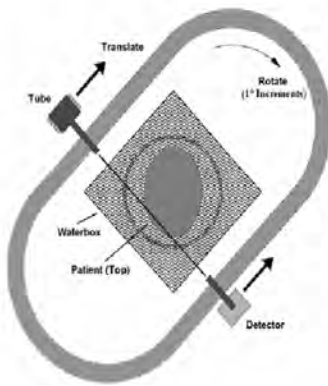


- Reconstruction methods based on Radon's work
  - 1917-classic image reconstruction from projections paper
- 1972 - Hounsfield develops the first commercial x-ray CT scanner

- Hounsfield and Cormack receive the 1979 Nobel Prize for their CT contributions
- Classical reconstruction is based on the Radon transform
  - Method known as backprojection
- Alternative approaches
  - Fourier Transform and iterative series-expansion methods
  - Statistical estimation methods
  - Wavelet and other multiresolution methods
  - Sub-Nyquist sampling: Compressed sensing and Partial Fourier Theories

# 1<sup>st</sup> Generation CT: Parallel Projections

## Hounsfield's Experimental CT



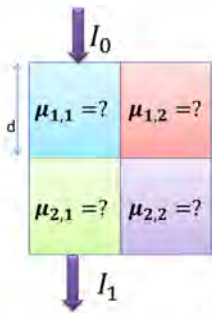
- 1 Beam and 1 Detector
- 160 samples/traverse: 5min
- 1° increments over 180°
- 28,800 samples
- Solved simultaneous equations (Fortran): **2.5h**
- $160^2$  image matrix but reduced to  $80^2$  for practical clinical use

# Example

$\mu_{1,1} = ?$	$\mu_{1,2} = ?$
$\mu_{2,1} = ?$	$\mu_{2,2} = ?$

Suppose an object that has 4 materials arranged in the boxes shown above. How can we find the linear attenuation coefficients?

# Image Reconstruction



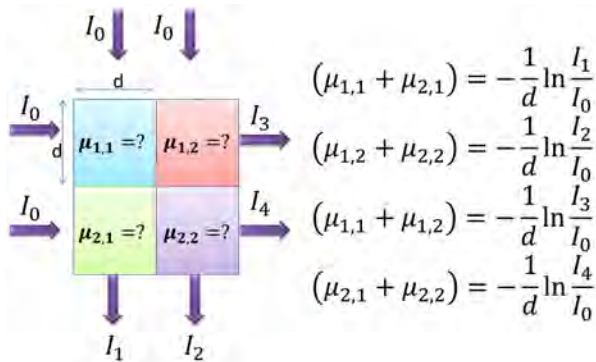
Suppose an x-ray of intensity  $I_0$  is passing through the first column of the object, and that  $I_1$  is the intensity measured at the other side.

$$I_1 = I_0 e^{-(\mu_{1,1} + \mu_{2,1})d}$$

$$\ln \frac{I_1}{I_0} = -(\mu_{1,1} + \mu_{1,2})d$$

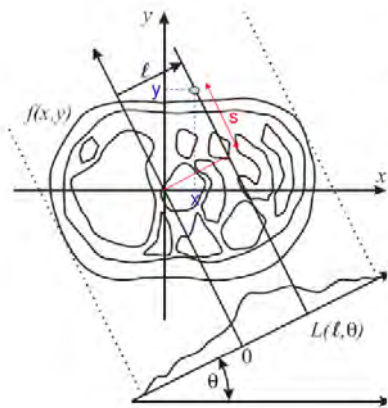
$$(\mu_{1,1} + \mu_{1,2}) = -\frac{1}{d} \ln \frac{I_1}{I_0}$$

# Image Reconstruction



If we repeat the same process for each of the rows and the columns, we obtain the equations necessary to obtain the values of the coefficients. However for bigger systems, the number of equations is not practical for implementation.

# Radon Transform

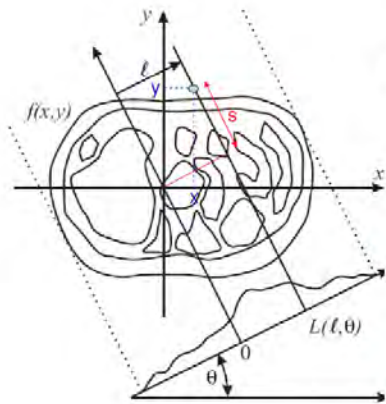


$f(x,y)$  describes our object

We would like to now describe  $f(x,y)$  in terms of its projections onto a line  $L(l,\theta)$ .

Here  $l$  is a distance along the line  $L(l,\theta)$  starting from the origin.

# Radon Transform



$f(x, y)$  describes our object

We would like to now describe  $f(x, y)$  in terms of its projections onto a line  $L(l, \theta)$ .

Here  $l$  is a distance along the line  $L(l, \theta)$  starting from the origin.

**Example: If  $\theta = 0$**

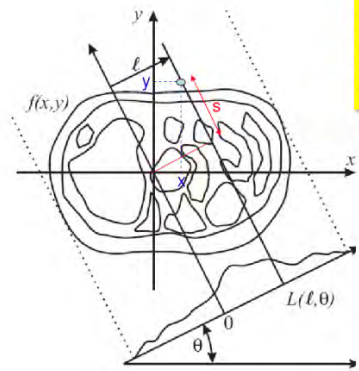
$$g(l, \theta = 0) = \int_{-\infty}^{\infty} f(l, y) dy$$

**Example: If  $\theta = 90^\circ$**

$$g(l, \theta = 90^\circ) = \int_{-\infty}^{\infty} f(x, l) dx$$

# Radon Transform

For Angles different to 0 or 90 degrees.



Option 1: We rotate our coordinate system so that  $l$  and the projection direction (axis of integration) are horizontal and vertical

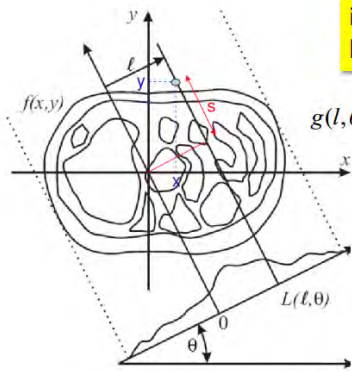
$$x(s) = l \cdot \cos(\theta) - s \cdot \sin(\theta)$$

$$y(s) = l \cdot \sin(\theta) + s \cdot \cos(\theta)$$

$$g(l, \theta) = \int_{-\infty}^{\infty} f(x(s), y(s)) ds$$

# Radon Transform

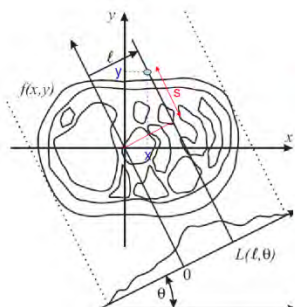
Option 2: Instead of rotating the object and integrating we can integrate the object only along the line (L)



$$g(l, \theta) = \int_{-\infty}^{\infty} \int_{-\infty}^{\infty} f(x, y) \cdot \delta(x \cos \theta + y \sin \theta - l) dx dy$$

$g(l, \theta)$  is called the Radon transform

# Radon Transform



$$x(s) = l \cdot \cos(\theta) - s \cdot \sin(\theta)$$

$$y(s) = l \cdot \sin(\theta) + s \cdot \cos(\theta)$$

$$g(l, \theta) = \int_{-\infty}^{\infty} f(x(s), y(s)) ds$$

How does this apply to xrays?

Recall that  $I_d = I_o e^{-\int_0^d \mu(x(s), y(s)) ds}$

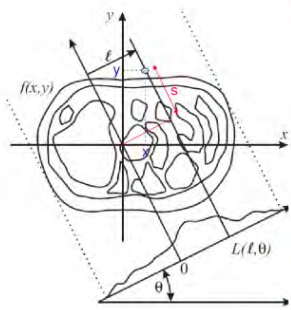
Is the received xray intensity of a beam that is projected through a sample along the line s

$$-\ln\left(\frac{I_d}{I_o}\right) = \int_0^d \mu(x(s), y(s)) ds$$

Let:  $g(l, \theta) = -\ln\left(\frac{I_d}{I_o}\right)$  and  $f(x, y) = \mu(x, y)$

we get the radon transform

# Radon Transform



Given  $g(l, \theta) = -\ln\left(\frac{I_d}{I_o}\right)$  and  $f(x, y) = \mu(x, y)$

$$x(s) = l \cdot \cos(\theta) - s \cdot \sin(\theta)$$

$$y(s) = l \cdot \sin(\theta) + s \cdot \cos(\theta)$$

$$g(l, \theta) = \int_{-\infty}^{\infty} f(x(s), y(s)) ds$$

In CT we measure  $g(l, \theta) = -\ln\left(\frac{I_d}{I_o}\right)$   
and need to find  $f(x, y) = \mu(x, y)$

using  $g(l, \theta) = \int_{-\infty}^{\infty} f(x(s), y(s)) ds$

$$x(s) = l \cdot \cos(\theta) - s \cdot \sin(\theta)$$

$$y(s) = l \cdot \sin(\theta) + s \cdot \cos(\theta)$$

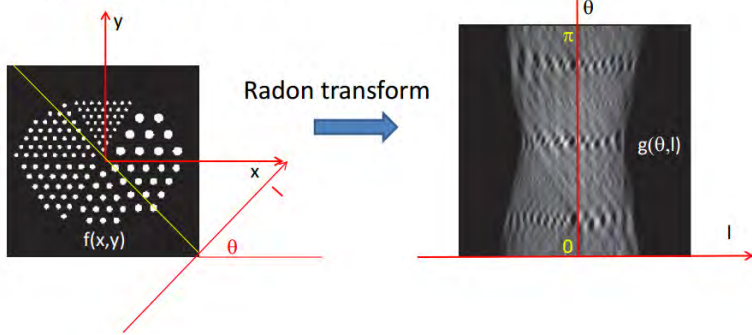
# Sinogram

A sinogram is an image of  $g(l, \theta)$

$$g(l, \theta) = \int_{-\infty}^{\infty} f(x(s), y(s)) ds$$

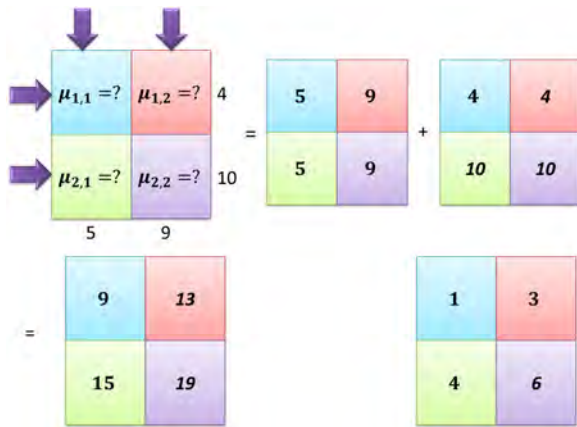
$$x(s) = l \cdot \cos(\theta) - s \cdot \sin(\theta)$$

$$y(s) = l \cdot \sin(\theta) + s \cdot \cos(\theta)$$



# Back Projection Example

With the example of the 4 boxes given before, we back project the results obtained. As it can be seen, the right answer is not obtained, however the order of the numbers is the same:



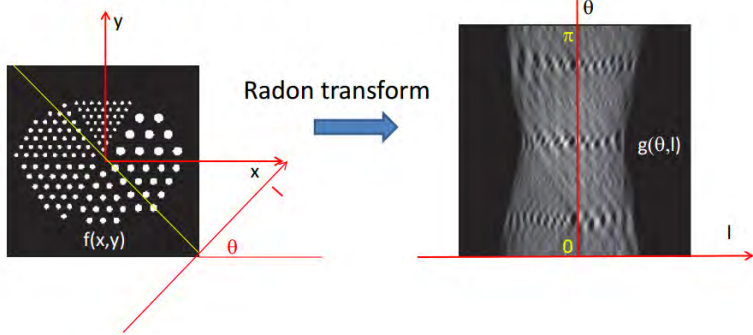
# Back Projection Method

A sinogram is an image of  $g(l, \theta)$

$$g(l, \theta) = \int_{-\infty}^{\infty} f(x(s), y(s)) ds$$

$$x(s) = l \cdot \cos(\theta) - s \cdot \sin(\theta)$$

$$y(s) = l \cdot \sin(\theta) + s \cdot \cos(\theta)$$

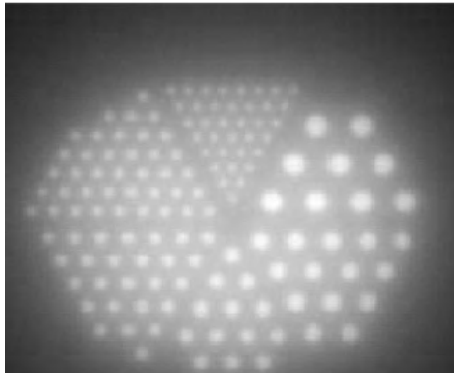


# Problems with Back Projection Method

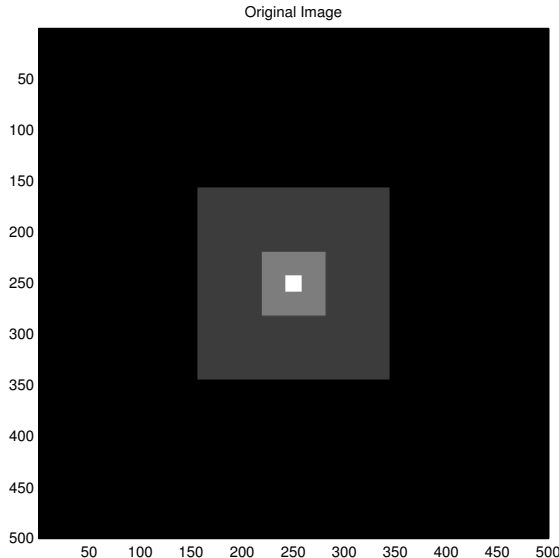
- Bright spots tend to reinforce, which results in a blurry image.
- Problem:

$$f_b(x, y) \neq f(x, y)$$

- Resulting Image:



# Back Projection Example

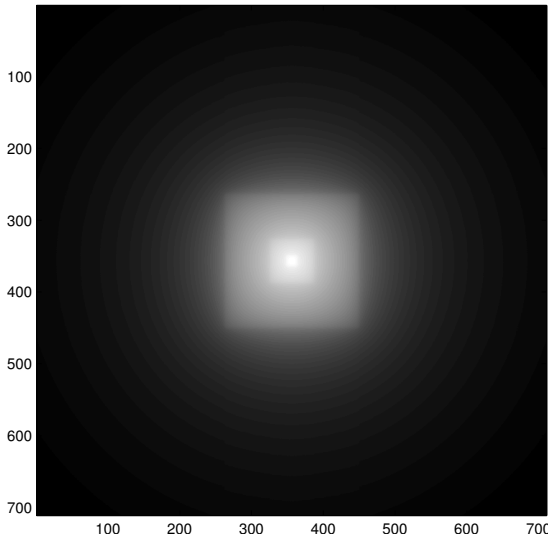


# Back Projection Example

(Loading Video...)

# Reconstruction: Back Projection

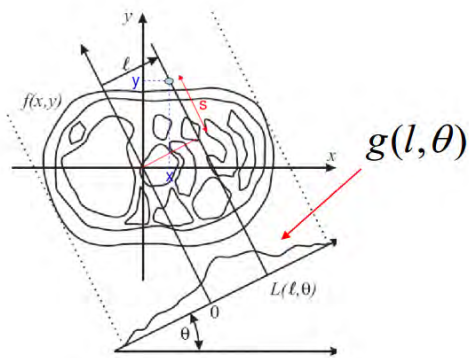
Result of the Backprojection algorithm



# Projection-Slice Theorem

First take the 1D Fourier transform of a projection  $g(l, \theta)$

$$G(\rho, \theta) = \mathfrak{I}_{1D} \{g(l, \theta)\} = \int_{-\infty}^{\infty} g(l, \theta) e^{-j2\pi\rho l} dl$$



# Projection-Slice Theorem

From the 1D Fourier transform of a projection  $g(l, \theta)$

$$G(\rho, \theta) = \mathfrak{I}_{1D}\{g(l, \theta)\} = \int_{-\infty}^{\infty} g(l, \theta) e^{-j2\pi\rho l} dl$$

Next we substitute the Radon transform for  $g(l, \theta)$

$$g(l, \theta) = \int_{-\infty}^{\infty} \int_{-\infty}^{\infty} f(x, y) \cdot \delta(x \cos \theta + y \sin \theta - l) dx dy$$

$$G(\rho, \theta) = \int_{-\infty}^{\infty} \int_{-\infty}^{\infty} \int_{-\infty}^{\infty} f(x, y) \cdot \delta(x \cos \theta + y \sin \theta - l) e^{-j2\pi\rho l} dx dy dl$$

Next we do a little rearranging

$$G(\rho, \theta) = \int_{-\infty}^{\infty} \int_{-\infty}^{\infty} f(x, y) \left\{ \int_{-\infty}^{\infty} \delta(x \cos \theta + y \sin \theta - l) e^{-j2\pi\rho l} dl \right\} dx dy$$

# Projection-Slice Theorem

$$G(\rho, \theta) = \int_{-\infty}^{\infty} \int_{-\infty}^{\infty} f(x, y) \left\{ e^{-j2\pi\rho[x\cos\theta + y\sin\theta]} \right\} dx dy$$

$$G(\rho, \theta) = \int_{-\infty}^{\infty} \int_{-\infty}^{\infty} f(x, y) \left\{ e^{-j2\pi[x\rho\cos\theta + y\rho\sin\theta]} \right\} dx dy$$

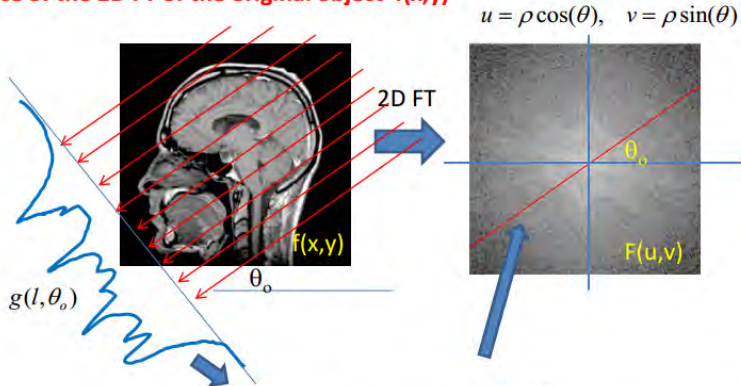
What does this look like?

This looks a lot like  $F(u, v) = \int_{-\infty}^{\infty} \int_{-\infty}^{\infty} f(x, y) e^{-j2\pi[xu + yv]} dx dy$

with  $u = \rho \cos(\theta)$ ,  $v = \rho \sin(\theta)$

# Projection-Slice Theorem

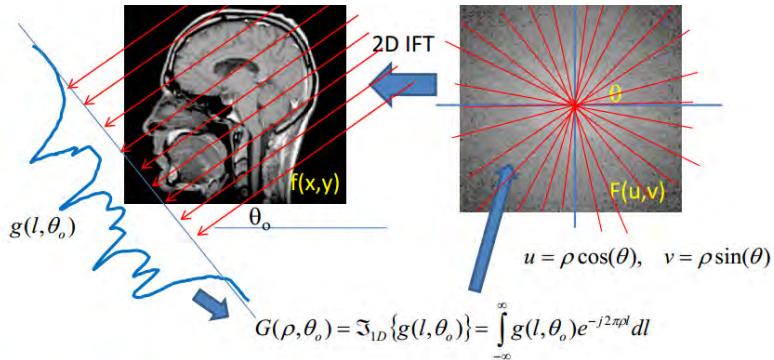
If I take the 1D FT of a projection at an angle  $\theta$  the result is the same as a slice of the 2D FT of the original object  $f(x,y)$



$$G(\rho, \theta_o) = \mathcal{F}_{1D}\{g(l, \theta_o)\} = \int_{-\infty}^{\infty} g(l, \theta_o) e^{-j2\pi \rho l} dl$$

$$u = \rho \cos(\theta), \quad v = \rho \sin(\theta)$$

# Fourier Reconstruction Method



Take projections at all angles  $\theta$ .

Take 1D FT of each projection to build  $F(u,v)$  one slice at a time.

Take the 2D inverse FT to reconstruct the original object based on  $F(u,v)$

$$f(x, y) = \mathfrak{I}_{2D}^{-1}\{G(\rho, \theta)\}$$

# Fourier Reconstruction Method

- The projection slice theorem leads to the following reconstruction method:
  - Take 1D Fourier Transform of each projection to obtain  $G(\rho, \theta)$  for all  $\theta$ .
  - Convert  $G(\rho, \theta)$  to Cartesian grid  $F(u, v)$ .
  - Take inverse 2D Fourier Transform to obtain  $f(x, y)$ .
- It is not used because it is difficult to interpolate polar data into a Cartesian grid, and the inverse 2D Fourier Transform is time consuming

# Filtered Back Projection

Consider the inverse Fourier Transform in 2D:

In polar coordinates the inverse Fourier transform can be written as

$$f(x, y) = \int_0^{2\pi} \int_{-\infty}^{\infty} F(\rho \cos \theta, \rho \sin \theta) e^{j2\pi\rho[x \cos \theta + y \sin \theta]} \rho d\rho d\theta$$

with  $u = \rho \cos(\theta)$ ,  $v = \rho \sin(\theta)$

From the projection theorem  $G(\rho, \theta) = F(\rho \cos(\theta), \rho \sin(\theta))$

We can write this as  $f(x, y) = \int_0^{2\pi} \int_{-\infty}^{\infty} G(\rho, \theta) e^{j2\pi\rho[x \cos \theta + y \sin \theta]} \rho d\rho d\theta$

# Filtered Back Projection

Since  $g(l, \theta) = g(-l, \theta + \pi)$  you can show

$$f(x, y) = \int_0^{\pi} \int_{-\infty}^{\infty} G(\rho, \theta) e^{j2\pi\rho[x\cos\theta + y\sin\theta]} |\rho| d\rho d\theta$$

which can be rewritten as

$$f(x, y) = \int_0^{\pi} \left[ \int_{-\infty}^{\infty} G(\rho, \theta) e^{j2\pi\rho l} |\rho| d\rho \right]_{l=x\cos(\theta) + y\sin(\theta)} d\theta$$

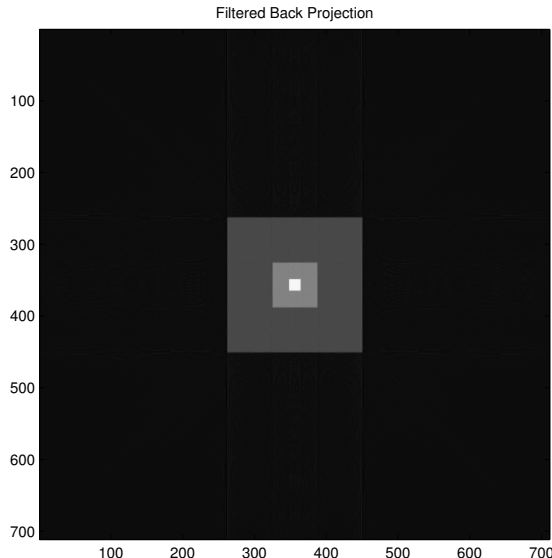
# Filtered Back Projection

- Filter Response.
  - $c(\rho) = |\rho|$ .
  - High pass filter.
- $G(\rho, \theta)$  is more densely sampled when  $\rho$  is small.
- The ramp filter compensates for the sparser sampling at higher  $\rho$ .

# Filtered Back Projection Example

(Loading Video...)

# Reconstruction: Filtered Back Projection



# Back Projection Method Vs Filtered Back Projection

## A. Back Projection

$$b_\theta(x, y) = g(x \cos(\theta) + y \sin(\theta), \theta)$$

$$f_b(x, y) = \int_0^\pi b_\theta(x, y) d\theta$$

## B. Filtered Back Projection

$$G(\rho, \theta) = \mathfrak{I}_{1D} \{g(l, \theta)\} = \int_{-\infty}^{\infty} g(l, \theta) e^{-j2\pi\rho l} dl$$

$$f(x, y) = \int_0^\pi \left[ \int_{-\infty}^{\infty} G(\rho, \theta) e^{j2\pi\rho l} |\rho| d\rho \right]_{l=x \cos(\theta) + y \sin(\theta)} d\theta$$

# Convolution Back Projection

From the filtered back projection algorithm we get

$$f(x, y) = \int_0^{\pi} \left[ \int_{-\infty}^{\infty} G(\rho, \theta) e^{j2\pi\rho l} |\rho| d\rho \right]_{l=x\cos(\theta)+y\sin(\theta)} d\theta$$

It may be easier computationally to compute the inner 1D IFT using a convolution

recall  $\mathfrak{I}_{1D}^{-1}[F_1(\omega) \cdot F_2(\omega)] = f_1(x) * f_2(x)$

$$\Rightarrow f(x, y) = \int_0^{\pi} \left[ g(l, \theta) * \mathfrak{I}_{1D}^{-1}(|\rho|) \right]_{l=x\cos(\theta)+y\sin(\theta)} d\theta$$

# Convolution Back Projection

$$f(x, y) = \int_0^{\pi} [g(l, \theta) * \mathfrak{I}_{1D}^{-1}(|\rho|)]_{l=x\cos(\theta)+y\sin(\theta)} d\theta$$

Let

$$c(l) = \mathfrak{I}_{1D}^{-1}(|\rho|)$$

$$f(x, y) = \int_0^{\pi} [g(l, \theta) * c(l)]_{l=x\cos(\theta)+y\sin(\theta)} d\theta$$

The problem is  $c(l) = \mathfrak{I}_{1D}^{-1}(|\rho|) = \int_{-\infty}^{\infty} |\rho| e^{j2\pi l\rho} d\rho$  does not exist

# Convolution Back Projection

The solution  $\tilde{c}(l) = \mathfrak{I}_{1D}^{-1}(|\rho| \cdot W(\rho)) = \int_{-\infty}^{\infty} |\rho| \cdot W(\rho) e^{j2\pi\rho l} d\rho$

where  $W(\rho)$  is called a weighting function

$$f(x, y) = \int_0^{\pi} [g(l, \theta) * \tilde{c}(l)] d\theta$$

$$\tilde{c}(l) = \mathfrak{I}_{1D}^{-1}(|\rho| \cdot W(\rho)) = \int_{-\infty}^{\infty} |\rho| \cdot W(\rho) e^{j2\pi\rho l} d\rho$$

# Convolution Back Projection

$$f(x, y) = \int_0^{\pi} [g(l, \theta) * \tilde{c}(l)] d\theta$$

$$\tilde{c}(l) = \mathfrak{I}_{1D}^{-1}(|\rho| \cdot W(\rho)) = \int_{-\infty}^{\infty} |\rho| \cdot W(\rho) e^{j2\pi \rho l} d\rho$$

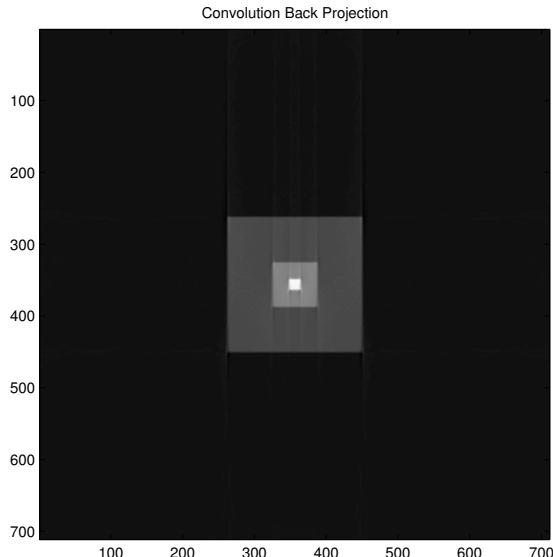
## Common windows

- Hamming window
- Lanczos window (Sinc function)
- Simple rectangular window
- Ram-Lak window
- Kaiser window
- Shepp-Logan window

# Convolution Back Projection Example

(Loading Video...)

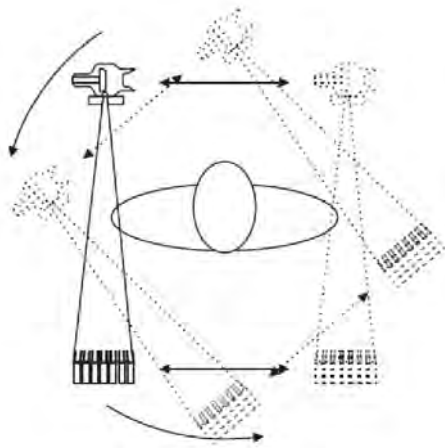
# Reconstruction: Convolution Back Projection



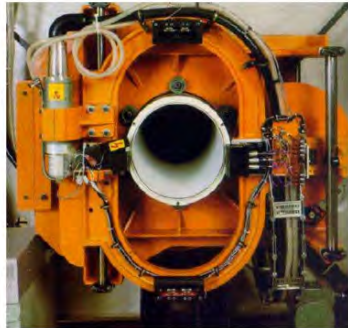


## 2<sup>nd</sup> Generation

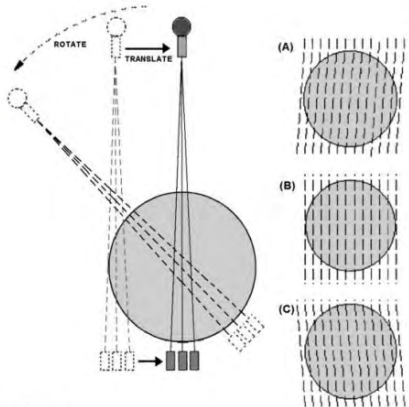
- Incorporated linear array of 30 detectors
- More data acquired to improve image quality
- Shortest scan time was 18 seconds/slice
- Narrow fan beam allows more scattered radiation to be detected



# 2<sup>nd</sup> Generation

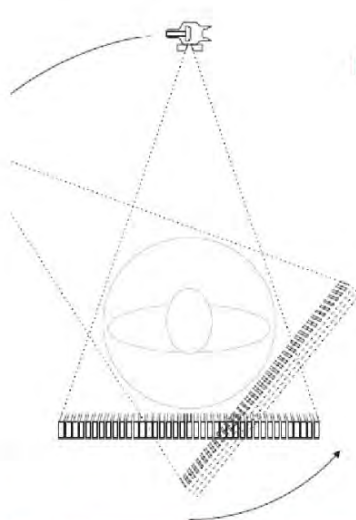


- Multiple detectors
- Still translate-rotate
  - 1 view acquired per detector ( $\sim 1^\circ$  apart)
  - angular increment increased by using more detectors



# 3<sup>rd</sup> Generation

- Number of detectors increased substantially (more than 800 detectors)
- Angle of fan beam increased to cover entire patient ( no need for translational motion)
- Mechanically joined x-ray tube and detector array rotate together
- Newer systems have scan times of 1/2 second



# 2<sup>nd</sup> and 3<sup>rd</sup> Generation Reconstructions

1972: 5 Minutes



1976: 2 Seconds

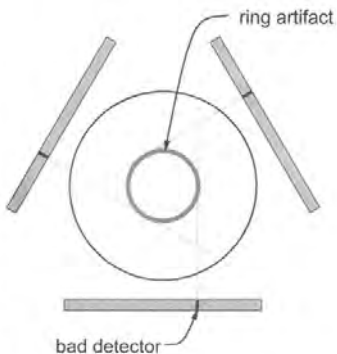
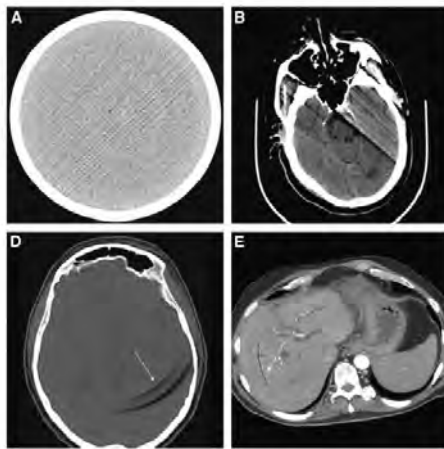


3G

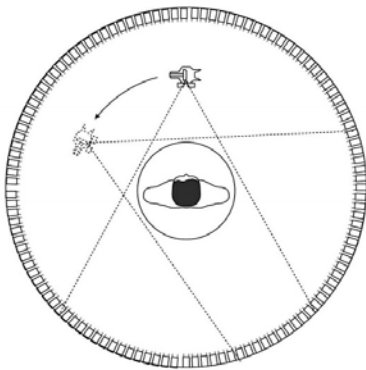


# 3<sup>rd</sup> Generation Artifacts

## Ring Artifacts



# 4<sup>rth</sup> Generation



Designed to overcome the problem of artifacts. Stationary ring of about 4800 detectors